

The Eurasia Proceedings of Science, Technology, Engineering & Mathematics (EPSTEM), 2024

Volume 32, Pages 476-482

IConTES 2024: International Conference on Technology, Engineering and Science

Assessment of Fatigue and Corrosion Effects on Coating from the SMAW Process

Djilali Allou

Research Center in Industrial Technologies (CRTI)

Sarra Djemmah

Research Center in Industrial Technologies (CRTI)
University of Mons

Youcef Faci

Research Center in Industrial Technologies (CRTI)

Rachid Amraoui

Research Center in Industrial Technologies (CRTI)

Abstract: This study examines how wear impacts the mechanical properties of the interface between weld overlay Inconel 182 and a 25CD4 substrate when using the SMAW process. The microstructure at the interface of the Inconel 182 /25CD4 substrate mainly featured columnar Ni- γ , with a gradient of Ni ;Cr and Fe, elements diffusing from the melting limits to the type II boundary close to the interface. A scratch resistance test was carried out on the interface to evaluate the adhesion and wear resistance of the Inconel 182 overlay and the 25CD4 substrate. The test was performed under a constant load of approximately 100 N, with a spherical indenter of 0.6 mm radius, creating a (5 mm) scratch length over a period of 50 s at a scratch speed (0.1 mm/s). There are two zones. A reloading zone (Inconel 182) with totally Viscoplastic contact another zone which is that of the substrate presenting elastic deformations at the same time. The variation of the coefficient of friction over time across the substrate/recharge interface reveals three distinct zones. The coefficient of friction increases rapidly until it reaches a maximum of 0.63, corresponding to a zone of high roughness (inter-diffusion zone). The electrochemical characteristics of the Inconel 182 overlay and the 25CD4 substrate in a 3.5% NaCl solution revealed evidence of galvanic corrosion.

Keywords: 25CD4, Corrosion, Wear, SMAW process, Inconel 182 weld overlay

Introduction

The oil industry relies on blowout preventers (BOPs) as part of well control equipment to shut down the well in case of a blowout (Han et al., 2015; Specification API, 2010). Xindu et al. has shown that both hard and soft shut-ins are viable options, but hard shut-ins are the fastest and safest method for closing the well (Han et al., 2013; Metals, 2000). During drilling operations, it is essential to regularly test the BOPs every 21 days to ensure they are functioning properly as safety devices, in compliance with (API 16A R and SP53), the American Petroleum Institute Code (Lyon et al., 2024; Specification API, 2010).

In the environment of drilling, the walls of the Blowout Preventer (BOP) are subordinated to specific service conditions, including dynamic stresses and climate. The walls of the Blowout Preventer (BOP) are exposed to colorful cyclic lading conditions during drilling. The pressure of the drilling fluid, climate, and shocks, the movement of the font, as well as contraction and bending forces are some of the main conditions they face (Su

- This is an Open Access article distributed under the terms of the Creative Commons Attribution-Noncommercial 4.0 Unported License, permitting all non-commercial use, distribution, and reproduction in any medium, provided the original work is properly cited.

- Selection and peer-review under responsibility of the Organizing Committee of the Conference

© 2024 Published by ISRES Publishing: www.isres.org

et al., 2018). The pressure of the fluid pumped into the well fluctuates at high pressure, causing repeated stress on the BOP's walls. The drill bit encountering different creates climate and shocks, generating cyclic tension cycles. also, the weight of the drilling outfit and rods exerts contraction and bending forces, applying cyclic stresses on the walls. (Jianhong et al., 2012).

Inconel 182 is a chromium, nickel, and iron-based alloy that is highly resistant to corrosion in harsh environments. It has excellent mechanical properties at high temperatures, making it suitable for use in the chemical and petrochemical industries for manufacturing heat exchangers and reactors. Steel 25CD4, on the other hand, is a chrome-molybdenum alloy steel with high mechanical strength, toughness, and hardness. It is known for its resistance to wear, fatigue, and stress corrosion cracking, and is widely used in the manufacturing of parts that are subjected to dynamic loads, such as transmission shafts and gears, as well as for equipment requiring high strength. This study examines the impact of wear and electrochemical behavior on the mechanical properties of the interface between a weld overlay of Inconel 182 and a 25CD4 substrate, using the SMAW process in a drilling environment.

Materials and Experimental Procedures

The weld overlaid used used in this work is Inconel 182, which is provided in the form of 3.2 mm diameter electrode and coated on the surface of 25CD4 substrate using arc welding (SMAW) process. The chemical compositions of the materials used in this study are shown in Table 1. For the deposition process, the Inconel 182 electrode was connected to the positive terminal (EP), while the workpiece (25CD4 substrate) was connected to the negative terminal. The welding process was performed in two passes, working at similar speeds, with the first pass using 170 A direct current (DC) mode at 33 V and the second pass using 220 A and 34 V. The microstructure evolution was analyzed and examined by ZEISS optical microscope. Scratch measurements were conducted to evaluate the mechanical properties across the Inconel 182 /steel substrate interface. The scratch obtained at the level of the substrate interface 25CD4/ recharged by Inconel 182 in the case of the SMAW process with a typical constant load scratching ~ 100 N, in contact with spherical indenter, of a radius of 06 mm, a scratcher length of 5 mm corresponding to 50s and a scraping speed of 0.1mm/s.

Table 1. Chemical composition of the substrate and the filler metal (wt.%)

Elements / Wt%	25CD4	Inconel 182
C	0.3	0.1
Ni	0.12	61
Cr	1.04	15
Mo	0.23	-----
Mn	0.56	8
Si	0.28	0.4
Cu	0.15	0.5
P	0.01	0.3
S	0.02	0.15
Fe	bal	bal

Electrochemical impedance spectroscopy (EIS) and potentiodynamic polarization curve measurements were performed using a PGSTAT302N potentiostat and an Autolab electrochemical analyzer from Metrohm using NOVA software. The potentiodynamic polarization curves were measured at a scan rate of 0.01 V/s. The curves provide information about the corrosion behavior and enable the determination of corrosion current and potential. The EIS measurements were performed in the frequency range of 100 kHz to 100 MHz with an amplitude of 0.01 V. EIS is a powerful technique for analyzing electrochemical processes occurring at metal-electrolyte interfaces.

Results and Discussion

Microstructural Evolution

Figure 1-a) shows a cross section of a weld with a layer thickness of 6 mm. Two distinct regions can be seen: the 25CD4 base material (dark area) and the Inconel 182 layer associated with the weld (white area). The slow cooling rate during deposition promotes the transformation of austenite in the 25CD4 matrix into pearlite (dark) and fine ferrite grains (white), resulting in a unique microstructure as shown in Figure 1-b).

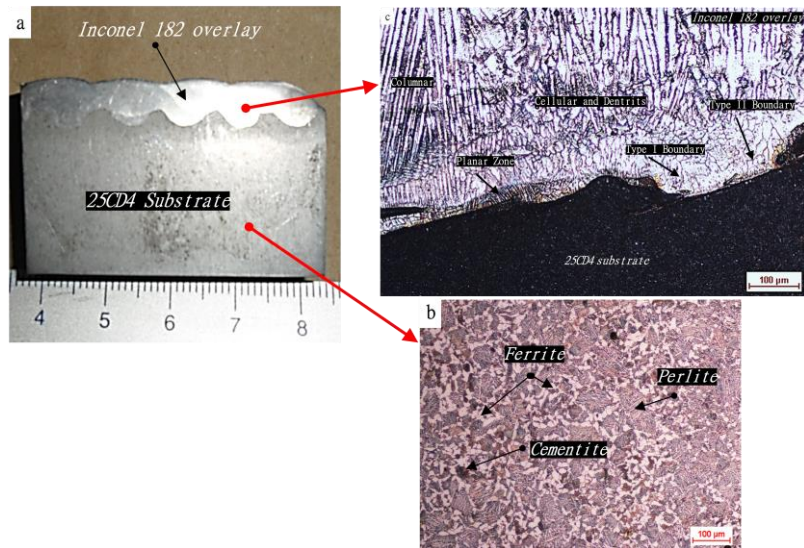


Figure 1. (a), Macrograph of weld overlaid Inconel 182 overlay/25CD4 substrate and optical Micrograph of different regions at the interface, fusion boundary zone: (b) 25CD4, (c) interface

Figure 1c shows the microstructure at the interface between the base material and the Inconel 182 coating. It is clear that the welded state exhibits a fine-grained structure, which is due to the high temperatures reached during welding. The microstructure of the Inconel 182 coating near the interface is shown in Figure 1c, showing the solidification morphology growing epitaxially from the steel-based interface towards the weld axis. This epitaxial growth corresponds to the planar region, which is characterized by the mixing of the chemical composition of the steel base with the Inconel elements, forming a thinning zone. This observation is consistent with previous studies (Allou et al.,2020; Bao et al.,2009; Tandon et al.,2020). The Inconel 182 overlay shows the creation of a Type I boundary, which follows the cooling direction and is aligned with the γ -structure (Shariatpanahi & Farhangi, 2010). As depicted in Figure 1c, the structure shifts from parallel to perpendicular to the line interface, forming a Type II boundary. Further away from the interface, a typical cellular-dendritic microstructure of Inconel 182 is visible.

Scratch Behavior

Figure 2 shows the MEB micrography of the scratch obtained at the level of the substrate interface 25CD4/ recharged by Inconel 182 in the case of the SMAW process with a typical constant load scratching ~ 100 N, in contact with spherical indenter, of a radius of 06 mm, a scratcher length of 5 mm corresponding to 50s and a scraping speed of 0.1mm/s.

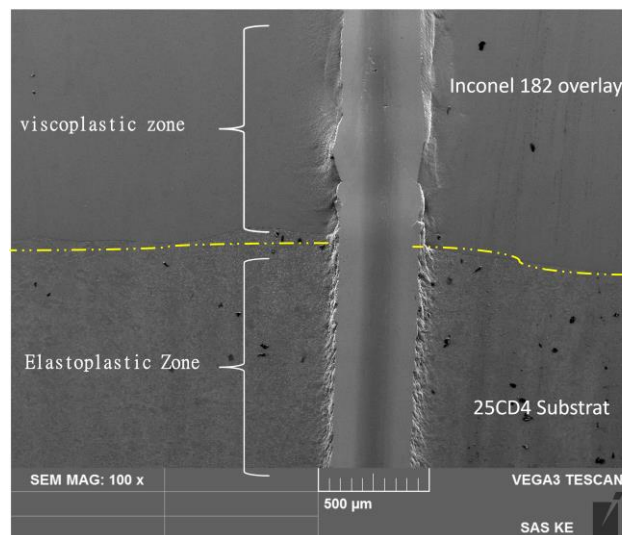


Figure 2. MEB micrography of the scratch obtained at the interface 25CD4/ recharged by Inconel 182 in the case of the SMAW process

Through this figure we can see the existence of two zones. A recharge area (Inconel 182) with a fully Viscoplastic contact with a very visible strip whose trajectory does not appear to be a perfect straight a separate non-symmetrical surface (half-circle) and another area that is that of the substrate with elastic deformations at the same time This type of contact, called plastic elastos, is caused by the appearance of fairly uniform side blades. The appearance of the secondary electron scratch at the level of the 25CD4/ interface for the SMAW process in strong magnification (Figure 2), the indenter footprint shows heterogeneous damage (different bottles) between the substrate and the recharge.

The flow of the material from both sides of the indenter takes place from the top to the bottom of the contact. Modes of deformation of the material, such as viscosity, plasticity, and friction, are involved, thus inducing an upward-down disymmetry of the contact and hence the formation of a residual rod because the material (fitting) is not elastic. We are in the presence of a plowing phenomenon; micro abrasion mechanisms appear. The upper part of the recharge is usually the most exposed to external aggression. We notice the presence of material pulling under a charge of 100 N (Figure 3).

The overlapping of the graphs of the variation of the friction coefficient depending on the time of the SMAW recharge through the substrate/recharge interface with the tangential forces ($F_z(N)$) are represented by figures 4. These graphs indicate the limit where the charge becomes constant and reaches 100 N. This configuration will allow us to delimit the end of zone 1. The graph of the variation of the coefficient of friction as a function of time across the substrate/load interface is shown in Figure 5, the curve presents three distinct zones.

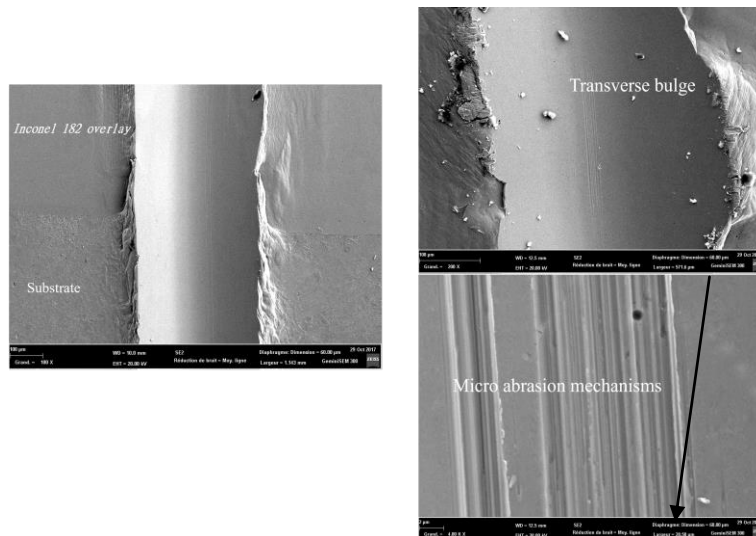


Figure 3. Appearance of the strip in e-secondary showing the emergence of the buffer, at the level of the interface

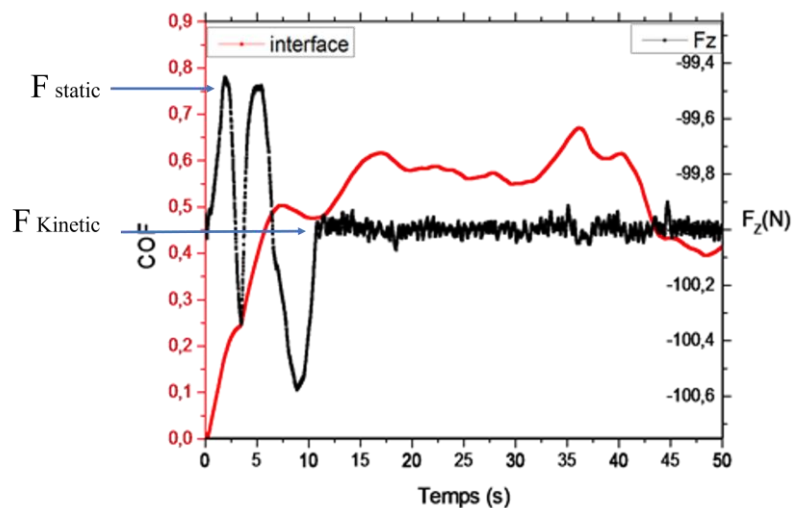


Figure 4. Superposition of the friction coefficient curves at the Substrate/ interface and the tangential force as a function of time (SMAW process)

Zone 1: Corresponds to the application of the load, where the coefficient of friction changes very rapidly. This increase is due to the presence of oxide and impurities, causing the indenter to undergo a frictional force during penetration, gradually reaching the depth of the scratch, with a coefficient of friction of 0.52 in 11 s.

Zone 2: represents the part of the substrate where the coefficient is fairly stable and constant, at around 0.55.

Zone 3: this is the resurfacing part; the coefficient of friction increases rapidly until it reaches a maximum of 0.63. This corresponds to a zone of high roughness (inter-diffusion zone). In adhesive mode, the curve falls gradually and stabilises at around 0.4. Referring to Figure 4, this value represents the upper part of the hardfacing. We note that in this zone, the curve takes on a downward trend, which seems to correspond to a sliding of the indenter without tearing of the material. In the specific case of our hardfacing, the coefficient of friction follows the trend of the hardness allocated to this hardfacing.

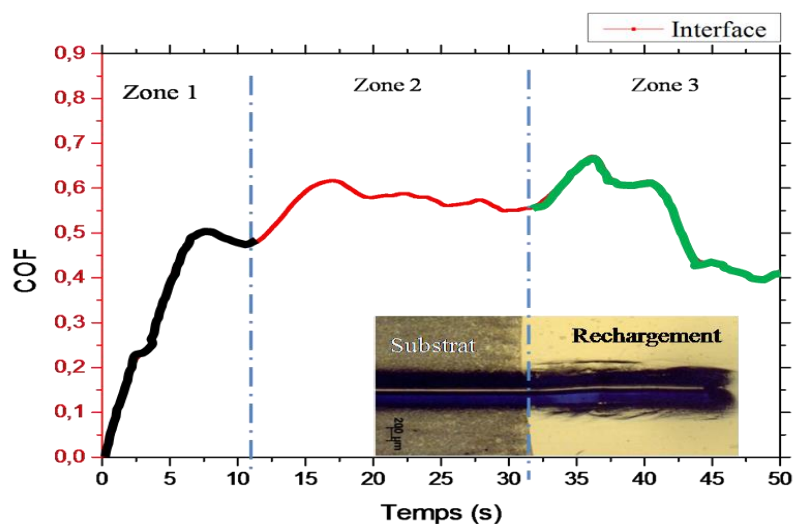


Figure 5. Curve of the coefficient of friction at the interface

Corrosion Behavior

Figure 6 shows the stacked polarisation curves for the system (substrate, interface and recharge) in a 3.5% NaCl-based electrolyte. They correspond to scan intervals between -1 and 0.1 V. The Ag/AgCl reference electrode was used for scan intervals between -0.6 and 0.4 V. We used a scan rate of 1mV/s from cathode to anode. Table 2 summarises the results of the polarisation curve in Figure 6 and shows the corrosion potential (E_{corr}), corrosion current density (i_{corr}) and corrosion rate.

Table 2. Electrochemical parameters of potentiodynamic tests

Eléments	Substrat	Interface Inconel 182 /25CD4	Reload
E_{corr} (MV)	-668	-626	-235
I_{corr} ($\mu\text{a}/\text{cm}^2$)	18,53	5,37	1,137
Corrosion rate (mm/year)	0,143	0,115	0,012

We observed a corrosion potential of -668 mV Ag/AgCl for the substrate and -235 mV Ag/AgCl for the Inconel 182 hard coating. The corrosion potential of the Inconel 182 interface/ substrate corresponds to an average value of -626 mV Ag/AgCl. This value is the point where the anode branch of the substrate intersects with the cathode branch of the hard facing.

Comparison of the average corrosion rates reinforces the choice of the hardfacing grade selected, as the corrosion rate of the base material (0.143 mm/yr) is higher than that of the Inconel182/base material interface (0.115 mm/yr) and the hardfacing (0.012 mm/yr). Galvanic corrosion, defined as corrosion between two materials with different potentials, follows the principle of a galvanic cell. The base material has a base potential (-668mV), while the overlay has the higher potential (-235mV), resulting in an increase in current flow. The average potential fluctuations (ΔE_{corr}) between base/recharge and base/interface are -433mV and -42mV respectively, with a ratio of one tenth.

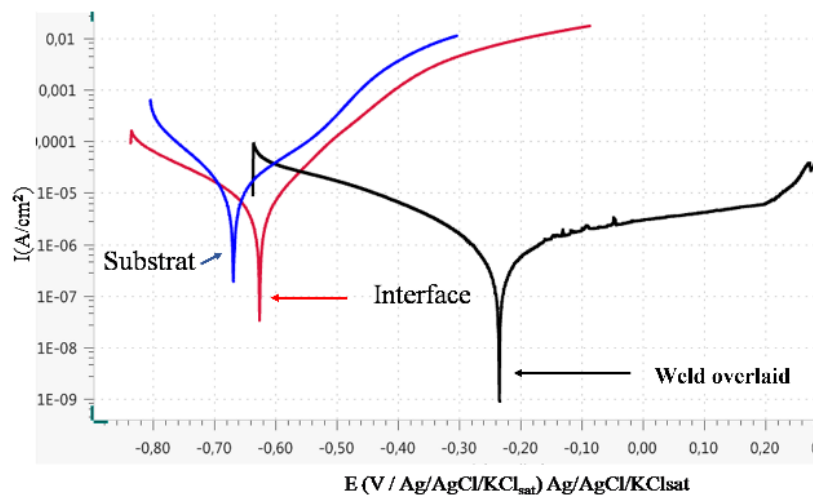


Figure 6. Superposition of the potentiodynamic curves

This indicates increased corrosion in a very hostile environment (3.5% NaCl). The dissimilar materials, 25CD4 substrate and Inconel 182 hardfacing, have different electrochemical potentials, which accelerates galvanic corrosion. The substrate acts as a sacrificial anode, causing it to degrade more rapidly than the hardfacing. Once the substrate degrades, the interface will be impacted. To prevent corrosion, including microscopic corrosion sites on the anode's surface, the metal couple requires a cathodic bias.

Conclusion

The effect of the impact of wear and electrochemical behavior on the mechanical properties of the interface between a weld overlay of Inconel 182 and a 25CD4 steel substrate is evaluated. The following conclusions can be drawn:

- Cross section of weld overlaid with a 6 mm layer thickness. Two distinct regions can be observed, the 25CD4 substrate (dark region) and the Inconel 182 layer referred to the weld overlay (white region).
- The friction coefficient depending on the time of the SMAW recharge through the substrate/recharge interface with the tangential forces ($F_z(N)$)
- The scratch obtained at the level of the substrate interface 25CD4/ recharged by Inconel 182 in the case of the SMAW process. we can see the existence of two zones. A recharge area (Inconel 182) with a fully Viscoplastic contact and another area that is that of the substrate with elastic deformations at the same time. This type of contact, called plastic elastos, is caused by the appearance of fairly uniform side blades
- The Inconel 182/substrate interface has a corrosion potential of around -626 millivolts, which is the point where the substrate's anode and the hardfacing's cathode meet. The existence of this galvanic cell at the interface speeds up the corrosion of the samples.

Scientific Ethics Declaration

The authors declare that the scientific ethical and legal responsibility of this article published in EPSTEM Journal belongs to the authors.

Acknowledgements or Notes

* This article was presented as a poster presentation at the International Conference on Technology, Engineering and Science (www.icontes.net) held in Antalya/Turkey on November 14-17, 2024.

* Thanks the Research Institute for Materials Science and Engineering

References

- Allou, D., Miroud, D., Ouadah, M., Cheniti, B., & Bouyegh, S. (2020). Criterion for cathodic protection of 25CD4/Inconel 182 system. *Applied Surface Science*, 502, 144100.
- Bao, G., Yamamoto, M., & Shinozaki, K. (2009). Precipitation and Cr depletion profiles of Inconel 182 during heat treatments and laser surface melting. *Journal of Materials Processing Technology*, 209(1), 416-425.
- Han, C., & Zhang, J. (2013). Study on well hard shut-in experiment based on similarity principle and erosion of ram rubber. *Engineering Failure Analysis*, 32, 202-208.
- Han, C., Yang, X., Zhang, J., & Huang, X. (2015). Study of the damage and failure of the shear ram of the blowout preventer in the shearing process. *Engineering Failure Analysis*, 58, 83-95.
- Jianhong, F., Kexiong, S., Zhi, Z., Dezhi, Z., Fei, L., Xin, X., & Xin, Z. (2012). Stress analysis on drilling string vibration in gas drilling. *Energy Procedia*, 16, 1264–1268.
- Lyons, W. C., & Plisga, G. J. (2004). *Standard handbook of petroleum and natural gas engineering* (2nd ed.). Elsevier.
- Metals, S. (2000). High-performance alloys for resistance to aqueous corrosion. *SM Aqueous Corrosion Book*, 28, 68.
- Shariatpanahi A, M., & Farhangi, H. (2010). Microstructure and mechanical properties of dissimilar ferritic and austenitic steel joints with an intermediate Inconel-182 buttering layer. *Advanced Materials Research*, 6, 449–456.
- Specification API. (2010). Specification for wellhead and christmas tree equipment. *API 6A*, 552(3), 10.
- Su, K., Butt, S., Yang, J., & Qiu, H. (2018). Coupled dynamic analysis for the riser-conductor of deepwater Surface BOP Drilling System. *Shock and Vibration*, 2018(1), 6568537.
- Tandon, V., Thombre, M. A., Patil, A. P., Taiwade, R. V., & Vashishtha, H. (2020). Effect of heat input on the microstructural, mechanical, and corrosion properties of dissimilar weldment of conventional austenitic stainless steel and low-nickel stainless steel. *Metallography, Microstructure, and Analysis*, 9, 668-677.

Author Information

Djilali Allou

Research Center in Industrial Technologies (CRTI), PB 64,
Chéraga, Algiers, Algeria.
Contact e-mail : djilallou@yahoo.fr

Sarra Djemmah

Research Center in Industrial Technologies (CRTI), PB 64,
Chéraga, Algiers, Algeria.

Youcef Faci

Research Center in Industrial Technologies (CRTI), PB 64,
Chéraga, Algiers, Algeria.

Rachid Amraoui

Research Center in Industrial Technologies (CRTI), PB 64,
Chéraga, Algiers, Algeria.

To cite this article:

Allou, D., Djemmah, S., Faci, Y., & Amraoui, R. (2024). Assessment of fatigue and corrosion effects on coating from the SMAW process. *The Eurasia Proceedings of Science, Technology, Engineering & Mathematics (EPSTEM)*, 32, 476-482.